



Full Text View

[Volume 30, Issue 1 \(January 2000\)](#)

Journal of Physical Oceanography

Article: pp. 31–39 | [Abstract](#) | [PDF \(160K\)](#)

Inertial Oscillations and Frontogenesis in a Zero Potential Vorticity Model

William Blumen

Program in Atmospheric and Oceanic Sciences, University of Colorado, Boulder, Colorado

(Manuscript received September 9, 1998, in final form December 17, 1998)

DOI: 10.1175/1520-0485(2000)030<0031:IOAFIA>2.0.CO;2

ABSTRACT

Geostrophic adjustment and frontogenesis are examined by means of a two-dimensional, inviscid, rotating and nonlinear fluid model that satisfies the condition of zero potential vorticity. The fluid is bounded top and bottom by level, rigid lids. The initial state is one of no motion, but an unbalanced horizontal temperature gradient is prescribed. The subsequent motion is represented as the sum of an inertial oscillation, with the frequency of the local Coriolis frequency f , and an evolving geostrophic flow. When a nondimensional parameter a , a Rossby number, satisfies $a < 1$, the gradient of the evolving geostrophic flow increases (frontogenesis) during the period $0 < t \leq \pi/f$; the gradient decreases during the period $\pi/f < t \leq 2\pi/f$ (frontolysis). When $a \geq 1$, the relative vorticity of the evolving geostrophic flow becomes infinite: a discontinuity forms at the top and bottom boundaries during the period $0 < t \leq \pi/f$. There is an equipartition of energy between the inertial oscillation and the geostrophic flow, and nonlinear interactions occur between them. An exact (Fourier) spectral representation of the solution on the bottom boundary is used to display the kinetic energy spectrum and the transfer of energy through the spectrum at the time that the discontinuity forms. Applications of the model to oceanic and to atmospheric frontogenesis and to restratification of the surface mixed layer, following a storm, are noted.

Table of Contents:

- [Introduction](#)
- [Model](#)
- [Solutions](#)
- [Energy and frontogenesis](#)
- [Final remarks](#)
- [REFERENCES](#)
- [APPENDIX](#)
- [FIGURES](#)

Options:

- [Create Reference](#)
- [Email this Article](#)
- [Add to MyArchive](#)
- [Search AMS Glossary](#)

Search CrossRef for:

- [Articles Citing This Article](#)

Search Google Scholar for:

- [William Blumen](#)

1. Introduction

The process of geostrophic adjustment has been examined by many investigators since [Rossby's \(1937\)](#) seminal study. The adjustment process following an initial mass imbalance is in itself a fundamental concept in the theory of geophysical fluid dynamics. Yet, many applications have emerged that are of importance in oceanic science. Among them are the relation between geostrophic adjustment and frontogenesis (e.g., [Ou 1984](#); [Blumen and Wu 1995](#)), surface mixed layer restratification following a storm (e.g., [Tandon and Garrett 1994, 1995](#)), and hydraulic jump or bore formation during adjustment (e.g., [Houghton 1969](#); [Kuo and Polvani 1997](#)). There are various other applications in the oceanic and

An hierarchy of models was proposed by [Blumen and Wu \(1995\)](#) to study geostrophic adjustment, all based on conservation of potential vorticity. The simplest, from both a mathematical and physical view, is the zero potential vorticity model (ZPV); next, the uniform potential vorticity model (UPV) contains the added feature of an ambient, uniform static stability field and is also analytically tractable: finally, the nonuniform potential vorticity model, although more realistic in application to the ocean or to the atmosphere, requires a numerical approach and is not considered. Blumen and Wu examined the final geostrophically adjusted state, for each of the ZPV and UPV models, which evolved from prescribed unbalanced initial states. The transient motions associated with either ZPV or with UPV were not taken into account. The mathematical approach was, in fact, the same one originally established by [Rossby \(1937\)](#) using a shallow-water model. The principal aim of the present study is to reexamine geostrophic adjustment as an initial-value problem, restricted to the ZPV model, in order to expose the transient motions and their effect on frontogenesis and on the adaptation to a balanced flow.

The ZPV model is probably the simplest nontrivial model of fluid flow in the presence of density or temperature gradients that can be devised. It is, however, not without interest. The model, introduced in [section 2](#), consists of fluid in uniform rotation about a vertical axis between two rigid lids. The flow is two-dimensional, nonlinear, and inviscid. The time-dependent solutions, displayed in [section 3](#), exhibit inertial oscillations at the Coriolis frequency f . The results presented extend the analyses by [Ou \(1984\)](#), [Blumen and Wu \(1995\)](#), and [Tandon and Garrett \(1994\)](#). It is demonstrated in [section 4](#) that the solution at a rigid boundary may be expressed as a Fourier cosine series, using [Platzman's \(1964\)](#) results, and from this solution the nonsteady energy spectrum and the transfer of energy through the spectrum may be derived. Some final remarks appear in [section 5](#). The principal results of this analysis are the demonstration that undamped inertial oscillations can exist in this nonlinear system, that the oscillation frequency is not altered by the frontogenesis that is taking place, and that a stationary, geostrophically balanced state is not achieved.

2. Model

The basic equations of two-dimensional, inviscid, and rotating flow are

$$\frac{\partial u}{\partial t} + u \frac{\partial u}{\partial x} + w \frac{\partial u}{\partial z} - fv = -\frac{\partial \pi}{\partial x}, \quad (1)$$

$$\frac{\partial v}{\partial t} + u \frac{\partial v}{\partial x} + w \frac{\partial v}{\partial z} + fu = 0, \quad (2)$$

$$0 = -\frac{\partial \pi}{\partial z} + g \frac{\theta}{\theta(0)}, \quad (3)$$

$$\frac{\partial u}{\partial x} + \frac{\partial w}{\partial z} = 0, \quad (4)$$

$$\frac{\partial}{\partial t} \frac{\theta}{\theta(0)} + u \frac{\partial}{\partial x} \frac{\theta}{\theta(0)} + w \frac{\partial}{\partial z} \frac{\theta}{\theta(0)} = 0, \quad (5)$$

where (u, \mathbf{v}, w) are velocity components in the usual (x, y, z) Cartesian coordinate directions, $\partial/\partial y \equiv 0$, $\pi = p/\rho(0)$ [p is the pressure and $\rho(0)$ is the reference density], $\theta/\theta(0)$ is the ratio of the temperature to a reference temperature, g is the acceleration of gravity, and the Coriolis parameter f is constant.

Three conservation principles that apply are conservation of potential vorticity, absolute linear momentum, and temperature, for example, [Blumen and Wu \(1995\)](#). Absolute momentum coordinates will be used. They are defined as

$$X = x + \mathbf{v}/f, \quad Z = z, \quad T = t, \quad (6)$$

where X is a conserved property of this system. The ‘‘momentum coordinates’’ [\(6\)](#) should not be confused with ‘‘geostrophic coordinates’’ introduced by [Eliassen \(1959\)](#) to study steady frontal circulations and by [Hoskins and Bretherton \(1972\)](#) to study frontogenesis in atmospheric flows. Geostrophic coordinates are defined with geostrophic velocities, but \mathbf{v} in [\(6\)](#) is the total meridional velocity; the sum of the geostrophic velocity \mathbf{v}_g and the ageostrophic velocity \mathbf{v}_a .

The potential vorticity q_0 , expressed by (1) in Blumen and Wu (1995), is also derived in momentum coordinates (11) as

$$q_0 = \left(1 - f^{-1} \frac{\partial v}{\partial X}\right)^{-1} \frac{\partial}{\partial Z} \frac{\theta}{\theta(0)},$$

where the Boussinesq approximation is employed, so that $\theta/\theta(0) \approx -\rho/\rho(0)$. The ZPV assumption, $q_0 = 0$, requires

$$\frac{\partial}{\partial Z} \frac{\theta}{\theta(0)} = 0. \quad (7)$$

Blumen and Wu show further that, since $\theta = \theta(X)$, the steady geostrophic flow may be expressed as

$$\mathbf{v}_g = -\frac{g}{f} \frac{\partial}{\partial X} \frac{\theta}{\theta(0)} \left(\frac{h}{2} - Z\right), \quad (8)$$

where the flow is confined to a channel, $0 \leq Z \leq h$. The time-dependent system, expressed by (1), (2), (4), and (5), is transformed into momentum coordinates in the appendix. This system of equations in momentum coordinates reduces to

$$\frac{\partial u_a}{\partial T} + w \frac{\partial u_a}{\partial Z} - f v_a = 0, \quad (9)$$

$$\frac{\partial v_a}{\partial T} + w \frac{\partial v}{\partial Z} + f u_a = 0, \quad (10)$$

$$\frac{\partial}{\partial X} \left(u_a + f^{-1} w \frac{\partial v}{\partial Z}\right) + \frac{\partial}{\partial Z} \left(1 - f^{-1} \frac{\partial v}{\partial X}\right) w = 0, \quad (11)$$

$$\frac{\partial}{\partial T} \frac{\theta}{\theta(0)} = 0, \quad (12)$$

where $u = u_a$ and $\mathbf{v} = \mathbf{v}_g + \mathbf{v}_a$. The subscript a denotes the ageostrophic component. A barotropic pressure gradient (independent of Z) should be retained on the right-hand side of (9) after geostrophic balance removes the Z -dependent part of the pressure gradient. According to Neves (1996), the pressure cannot be determined from the hydrostatic equation, since the pressure is not known at any level between the rigid lids. Neves neglects the barotropic pressure gradient, determines a solution, and then adjusts his numerical solution to ensure that the mass flux is constant in space and independent of time. The analytical solution obtained from (9) and (10) will be shown to satisfy these constraints.

Equations (7) and (12) show that $\theta/\theta(0)$ is only a function of X . The remaining equations may now be expressed as

$$\frac{\partial u^*}{\partial T} - f v^* = \frac{\partial}{\partial T} \frac{w}{f} \frac{\partial v}{\partial Z}, \quad (13)$$

$$\frac{\partial v^*}{\partial T} + f u^* = -\frac{\partial}{\partial T} \frac{w}{f} \frac{\partial u_a}{\partial Z}, \quad (14)$$

$$\frac{\partial u^*}{\partial X} + \frac{\partial w^*}{\partial Z} = 0, \quad (15)$$

where

$$\left. \begin{aligned} v^* &= v_a - f^{-1}w\partial u_a/\partial Z \\ w^* &= w(1 - f^{-1}\partial v/\partial X) \end{aligned} \right\}. \quad (16)$$

These starred variables are defined as in [Hoskins and Draghici \(1977\)](#) but, in this case, $\mathbf{v} = \mathbf{v}_g + \mathbf{v}_a$. Elimination of \mathbf{v}^* between [\(13\)](#) and [\(14\)](#) yields

$$\frac{\partial^2 u^*}{\partial T^2} + f^2 u^* = \frac{\partial}{\partial T} \left(\frac{\partial}{\partial T} \frac{w}{f} \frac{\partial v}{\partial Z} - w \frac{\partial u_a}{\partial Z} \right). \quad (17)$$

A vertical integration of [\(15\)](#), denoted by an overbar, gives

$$\frac{\partial \overline{u^*}}{\partial X} = 0, \quad (18)$$

where $w^* = 0$ at $Z = 0, h$. Next [\(17\)](#) is integrated over Z and [\(18\)](#) is applied to the result to obtain

$$0 = \frac{\partial^2}{\partial X \partial T} \left(\frac{\partial}{\partial T} \overline{\frac{w}{f} \frac{\partial v}{\partial Z}} - \overline{w \frac{\partial u_a}{\partial Z}} \right). \quad (19)$$

[Equation \(19\)](#) will be satisfied by the choice, without the bar average,

$$\frac{\partial}{\partial T} \frac{w}{f} \frac{\partial v}{\partial Z} - w \frac{\partial u_a}{\partial Z} = 0. \quad (20)$$

This latter condition [\(20\)](#) may also be expressed as

$$\frac{\partial}{\partial T} (u^* - u_a) + f(v^* - v_a) = 0. \quad (21)$$

The solutions, to be determined, will have the property that the vertically integrated mass flux, proportional to $\overline{u^*}$, is independent of both X and T . Then the barotropic pressure gradient, neglected in [\(9\)](#) or [\(13\)](#), does not become a factor in the analysis. Further simplification is possible by introduction of [\(20\)](#) into the right-hand side of [\(13\)](#). Then [\(13\)](#) and [\(14\)](#) may be expressed as

$$\frac{\partial u^*}{\partial T} - f v_a = 0, \quad (22)$$

$$\frac{\partial v_a}{\partial T} + f u^* = 0, \quad (23)$$

which will determine v_a and u^* . The geostrophic flow v_g is provided by [\(8\)](#) and w^* is determined from [\(15\)](#). The variables (u^*, w^*) require interpretation.

Consider the temperature [equation \(5\)](#) and express $\partial[\theta/\theta(0)]/\partial z$ using momentum coordinates as


$$\frac{\partial}{\partial z} \frac{\theta}{\theta(0)} = \frac{\partial}{\partial Z} \frac{\theta}{\theta(0)} + \frac{\partial}{\partial X} \frac{\theta}{\theta(0)} \frac{1}{f} \frac{\partial v}{\partial z}. \quad (24)$$

Further, [\(6\)](#) may be used to show that

Introduction of (7) and (25) into (24), and then into (5), reveals that

$$\frac{\partial \theta}{\partial t} \frac{\theta}{\theta(0)} + u^* \frac{\partial \theta}{\partial x} \frac{\theta}{\theta(0)} = 0. \quad (26)$$

The horizontal velocity u^* defined by (16), may be interpreted as an “effective” advection velocity—in effect, vertical advection may be incorporated into horizontal advection in this ZPV flow.

Figure 1  may be used to provide a geometric interpretation of w^* . The slanting thick solid line represents a surface $X = \text{const}$, or equivalently a temperature surface. The trigonometric relationships are

$$\left. \begin{aligned} \sin\phi &= dX/dx = 1 + f^{-1}\partial v/\partial x \\ \cos\phi &= dX/dz = f^{-1}\partial v/\partial z \end{aligned} \right\}. \quad (27)$$

Consider the projections of w and of $u^* - u_a$ onto an X surface:

$$\begin{aligned} w \sin\phi + (u^* - u_a) \cos\phi &= w \sin\phi \left[1 + \left(f^{-1} \frac{\partial v}{\partial z} \right)^2 \right] \\ &= w \sin\phi [1 + (\cot\phi)^2] \\ &= w/\sin\phi = w^*, \end{aligned} \quad (28)$$

where

$$\frac{1}{f} \frac{\partial v}{\partial z} = \left(1 - \frac{1}{f} \frac{\partial v}{\partial X} \right)^{-1} \frac{1}{f} \frac{\partial v}{\partial Z} \quad (29a)$$

and

$$\left(1 - \frac{1}{f} \frac{\partial v}{\partial X} \right)^{-1} = 1 + \frac{1}{f} \frac{\partial v}{\partial x}. \quad (29b)$$

The variable w^* represents forced motion directed along X or $\theta/\theta(0)$ surfaces.

3. Solutions

a. Analytical representation

Solutions of (22) and (23) are

$$\begin{aligned} u^* &= A_1 \sin fT + B_1 \cos fT, \\ v_a &= A_2 \sin fT + B_2 \cos fT, \end{aligned} \quad (30)$$

where the (A_i, B_i) are constants. The initial conditions are as given in Blumen and Wu (1995). They are expressed in terms of the present variables as

$$u^* = w^* = \mathbf{v}_g + \mathbf{v}_a = 0, \quad T = 0, \quad (31)$$

and $\theta/\theta(0)$ is only a function of the initial coordinate x_0 . The momentum coordinate X is related to x_0 by

$$X = x + \mathbf{v}/f = x_0 \quad (32)$$

as a consequence of its conservation property and initial condition (31). Both the horizontal and vertical structure of \mathbf{v}_a will be that of \mathbf{v}_g , given by (8). Then the solutions that satisfy (31) may be expressed as

$$v = -\frac{g}{f} \frac{\partial}{\partial x_0} \frac{\theta}{\theta(0)} \left(\frac{h}{2} - Z \right) (1 - \cos fT), \quad (33)$$

$$u^* = \frac{g}{f} \frac{\partial}{\partial x_0} \frac{\theta}{\theta(0)} \left(\frac{h}{2} - Z \right) \sin fT, \quad (34)$$

$$w^* = -\frac{1}{2} \frac{g}{f} \frac{\partial^2}{\partial x_0^2} \frac{\theta}{\theta(0)} Z (h - Z) \sin fT, \quad (35)$$

where $\partial/\partial X = \partial/\partial x_0$. Note that (18) is satisfied by u^* , given by (34), and $\theta/\theta(0)$ will be chosen to be periodic in X : the mass flux conditions are exactly satisfied. The actual velocities (u_a , w), to be displayed in physical space are, however, given by

$$u_a = u^* - f^{-1} w \partial v / \partial Z, \quad (36)$$

$$w = \left(1 - f^{-1} \frac{\partial v}{\partial X} \right)^{-1} w^*. \quad (37)$$

These velocities can be evaluated by means of (33)–(35).

It is interesting to analyze the present results before specification of $\theta/\theta(0)$. The representation by the starred variables shows that the motion undergoes an inertial oscillation, but the representation by (36) and (37) exhibits more than one frequency. The situation displayed here is akin to the situation that develops when describing the motion of, for example, coupled linear oscillators (Morse and Ingaard 1968). Transformation to normal coordinates, in the latter case, provides a description of the motion in terms of the natural frequencies of oscillation as if the oscillators are uncoupled; otherwise the motion is described by sums and differences of the natural frequencies as a measure of the coupling between the oscillators.

The ZPV model solution in which the end state is specified to be steady geostrophic balance (8) has been examined by Blumen and Wu (1995). Consideration of the time-dependent solution, (33)–(35), reveals that an undamped and nondispersive inertial oscillation must be included in specification of the complete solution. The nonlinear transformation, expressed by (32), contains the mechanism to concentrate gradients—frontogenesis. As a consequence, a steady balanced geostrophic flow is not realized as an end state in this ZPV model. It will be shown in section 3b that, depending on the initial conditions, either the relative vorticity becomes infinite in a finite time or that the solution is represented as the sum of a steady geostrophic part and a time-dependent inertial oscillation for all time. In this latter case, both frontogenesis and frontolysis occur during one inertial period.

The time-dependent motion treated by Tandon and Garrett (1994) corresponds to $\partial[\theta/\theta(0)]/\partial x_0 = \text{const}$, which results in $w^* = w = 0$ and $u^* = u_a$. As time progresses, the $\theta/\theta(0)$ surfaces tilt from the vertical (to be shown) and the fluid becomes vertically stratified. When $\partial[\theta/\theta(0)]/\partial x_0 \neq \text{const}$, $w^* \neq 0$ and frontogenesis will take place during the first half-cycle of an inertial oscillation. It is interesting to note, however, that this system, (33)–(35), does not exhibit buoyancy oscillations in association with the vertical stratification that develops. The “vertical motion” w^* represents a forced motion at the inertial frequency that always remains parallel to the isotherms. The (u_a , w) circulation, will, however, be shown to be a counterclockwise circulation that is consistent with the tilting of the isotherms.

b. Numerical representation

The initial temperature field will now be specified as

$$\theta/\theta(0) = Y \sin kx_0, (38)$$

where (Y, k) are respectively the amplitude and the wavenumber. Evaluations will be carried out using nondimensional quantities:

$$\left. \begin{aligned} x'_0 &= \lambda^{-1}x_0, & z' &= h^{-1}z, & t' &= ft, \\ (u', v') &= (g^*h)^{-1/2}(u_a, v), & w' &= (fh)^{-1}w \end{aligned} \right\} (39)$$

where $g^* = gY$ and $\lambda = (g^*h)^{1/2}f^{-1}$. The temperature in (38) may be expressed as

$$\Theta^{-1} \frac{\theta}{\theta(0)} = \sin ax'_0, (40)$$

where the parameter $a = \lambda k$ may be interpreted as a Rossby number. Hereafter the prime notation will be dropped.

The parameter range for the present evaluations is $a \leq 1$, which encompasses both inertial oscillations and frontogenesis. As demonstrated in [Blumen and Wu \(1995\)](#), temperature and velocity discontinuities occur when $1 - f^{-1}\partial\mathbf{u}/\partial X = 0$ [see (29b)]. Evaluation is carried out by use of (33), noting that $\partial/\partial X = \partial/\partial x_0$. The result shows that $a = 1$ is a critical value when the temperature field is expressed by (40): a discontinuity does not form when $a < 1$. When $a = 1$, a discontinuity occurs simultaneously at both lids at positions $|x| = \pi/2$ at time $t = \pi$, that is, at the end of the first half cycle of the inertial period. When $a > 1$, discontinuities will occur at the lids at various locations $|ax_0| < \pi/2$ and at times $t < \pi$.

The numerical procedure requires evaluation of (32) expressed as

$$x = x_0 + a \cos ax_0 \left(\frac{1}{2} - z \right) (1 - \cos t), (41)$$

where the initial temperature field is represented by (40). Each isotherm is vertical at $t = 0$. Horizontal advection commences when $t > 0$, according to (41). The sequence of tilting and frontogenesis is shown for two times in the left panel of [Fig. 2](#) for $a = 1$. The right panels show the alongfront velocity \mathbf{u} , which also develops discontinuities at both lids $|x| = \pi/2$ at time $t = \pi$. The plots for $a < 1$ (not shown) depict similar patterns, but discontinuity formation does not occur, and the pattern reverses when $t > \pi$ to recover the initial state at $t = 2\pi$.

The streamfunctions, defined by $u = -\Psi_z$ and $w = \Psi_x$, are displayed in [Fig. 3](#). The flow is counterclockwise in agreement with the tilt of the isotherms in [Fig. 2](#). Both (u, w) reduce to zero at $t = \pi$, and the ageostrophic circulation reverses direction when $\pi < t \leq 2\pi$.

[Figure 4](#) contains plots of (u, w) as functions of time at $x = \pi/4$. Three levels are displayed, $z = 0.25, 0.50,$ and 0.75 . These plots are the physical space (x, z, t) nondimensional representations of (36) and (37). The inertial oscillation is the most distinctive feature, but the effect of the higher harmonics is particularly noticeable at $z = 0.25$. The asymmetry in between $z = 0.25$ and $z = 0.75$ is associated with $w > 0$ at each level, but u^* reverses sign at $z = 0.5$.

4. Energy and frontogenesis

It is generally very difficult to examine the complex interactions that take place between quasi-balanced low frequency motions and unbalanced flows that may encompass a broad region of the oceanic and atmospheric frequency spectrum. A two timescale analysis is, however, appropriate when the unbalanced motions are restricted to high frequencies, and a well-defined (time) scale separation exists. This approach has been used by [Blumen \(1972\)](#) and by [Dewar and Killworth \(1995\)](#) to study the interactions between quasigeostrophic flows and gravity-inertia waves and by [Blumen \(1997\)](#) to examine how semigeostrophic frontogenetic flows interact with high frequency waves. In each case, the lowest order in the two timescale expansion procedure reveals that the fast motions undergo an amplitude modulation by the slowly evolving quasi-balanced flow. Since the slow motions conserve energy independently, energy is not transferred to the fast waves by this modulation of the amplitude.

The present model provides a relatively simple framework to analyze the interaction between the evolving geostrophic flow and the inertial oscillations. This analysis will be restricted to the bottom level surface at $z = 0$. The advantage is that the effect of the interaction between these two different flows on frontogenesis may also be examined.

The relevant equations are (1) and (2), with the barotropic pressure gradient omitted, expressed as

$$\frac{\partial u_a}{\partial t} + u_a \frac{\partial u_a}{\partial x} - f v_a = 0, \quad (42)$$

$$\frac{\partial v}{\partial t} + u_a \frac{\partial v}{\partial x} + f u_a = 0. \quad (43)$$

The solutions are (33) and (36), expressed in (x, t) space as

$$v = v_g + v_a = v_g(1 - \cos ft), \quad (44)$$

$$u_a = -v_g \sin ft, \quad (45)$$

where $\mathbf{v}_g = \mathbf{v}_g(x, t)$ and $\mathbf{v}_g(x, 0) = -(g^*hk/2f) \cos kx$ [$g^* = gY$, as in (39)]. Substitution of (44) and (45) into either (42) or (43) yields

$$\frac{\partial v_g}{\partial t} + u_a \frac{\partial v_g}{\partial x} = 0. \quad (46)$$

There is a mutual interaction: the geostrophic flow modulates the inertial oscillation, and the inertial oscillation affects the evolution of the geostrophic flow.

An energy equation for the oscillatory motion can be derived by multiplication of (42) and (43), respectively, by u_a and by v_a . Addition of these expressions and use of (46) provides

$$\frac{\partial}{\partial t} \frac{u_a^2 + v_a^2}{2} + u_a \frac{\partial}{\partial x} \frac{u_a^2 + v_a^2}{2} = 0. \quad (47)$$

Multiplication of (46) by \mathbf{v}_g yields

$$\frac{\partial}{\partial t} \frac{v_g^2}{2} + u_a \frac{\partial}{\partial x} \frac{v_g^2}{2} = 0. \quad (48)$$

The relationship $\mathbf{v}_g^2 = \mathbf{v}_a^2 + u_a^2$ is extracted from (44) and (45), and (47) and (48) may be expressed as

$$\frac{\partial}{\partial t} \frac{u_a^2 + v_a^2}{2} = \frac{\partial}{\partial t} \frac{v_g^2}{2}. \quad (49)$$

The equipartition of energy between the oscillations and the geostrophic flow, introduced at the initial time (31), is maintained for all time.

Further aspects of the energetics may be examined by means of (46). Substitution of (45) into (46) gives

$$\left(\frac{\partial}{\partial \tau} - v_g \frac{\partial}{\partial x} \right) v_g = 0, \quad (50)$$

where $\tau = f^{-1}(1 - \cos ft)$. This expression (50) is a well-studied nonlinear advection equation for the determination of \mathbf{v}_g ,

for example, [Platzman \(1964\)](#). The time and place of the formation of a discontinuity in \mathbf{v}_g , found in [section 4](#), may also be determined from [\(50\)](#). The manner in which the inertial oscillation affects the geostrophic flow, and frontogenesis, can be absorbed into τ , an independent time variable. The solution for \mathbf{v}_g , which satisfies the initial condition [\(38\)](#), may be expressed as ([Platzman 1964](#))


$$\mathbf{v}_g = -4(g^*h)^{1/2}a \sum_{n=1}^{\infty} (nf\tau)^{-1} J_n(nf\tau) \cos nkx, \quad (51)$$

where a is defined below [\(40\)](#) and J_n represents the Bessel function of order n . The inertial oscillation (u_a , \mathbf{v}_a) may be expressed similarly by use of [\(33\)](#) and [\(36\)](#). The expression in [\(51\)](#) is a convenient analytic representation for further analysis. [Platzman \(1964\)](#) has shown, from [\(51\)](#), that the energy spectrum $V(n)$ has the distribution

$$V(n) \sim n^{-8/3} \quad (52)$$

as $\tau \rightarrow \tau_c$, where τ_c is the time that a discontinuity forms. Further, the transfer of kinetic energy through the spectrum \mathcal{E}_n satisfies

$$n\mathcal{E}_n \approx \text{const} \quad (53)$$

as $\tau \rightarrow \tau_c$. These results [\(52\)](#) and [\(53\)](#) provide limiting values; that is, they apply for example to [Fig. 2](#) , where $a = 1$ and $ft \rightarrow \pi$ ($f\tau \rightarrow 2$).

When $a < 1$, the system undergoes an undamped inertial oscillation in cooperation with frontogenesis during the first half of the cycle, $0 \leq ft \leq \pi$. During this part of the cycle the relative vorticity $\partial\mathbf{v}_g/\partial x$ increases, and energy is transported downscale; the spectral slope approaches [\(52\)](#) but remains steeper. During the second half of the cycle, $\pi < ft \leq 2\pi$, a reversal occurs and the initial state is recovered when ft reaches the end of the first cycle at $ft = 2\pi$. When $a > 1$, a discontinuity develops ($\partial\mathbf{v}_g/\partial x = \infty$) at both lids during the first half of the cycle, $ft \leq \pi$. The energy spectrum and spectral transfer are as given by [\(52\)](#) and [\(53\)](#).

5. Final remarks

The ZPV model has been used primarily to examine frontogenesis ([Hoskins and Bretherton 1972](#); [Ou 1984](#); [Blumen and Wu 1995](#)) and mixed layer restratification ([Tandon and Garrett 1994](#)). In this model the temperature (or density) and absolute linear momentum surfaces coincide for all time, although these surfaces will tilt from a vertical orientation and move relative to each other, for example, frontogenesis. The lack of an ambient vertical stratification, as in a ZPV model, eliminates internal gravity waves and buoyancy oscillations as solutions. Inertial oscillations and frontogenesis (or frontolysis) represent the nonsteady response to unbounded initial conditions. The mathematical and physical simplicity of the ZPV model makes it an attractive starting point to gain insights about the complex dynamics of models of geophysically relevant flows.

The present analysis takes advantage of the mathematical simplicity of the ZPV model to provide a nonlinear, time-dependent, analytic solution of the fluid response to an initially imposed horizontal temperature gradient. Previous analyses of the ZPV model either do not consider the time-dependent motions, although nonlinearity is retained ([Ou 1984](#); [Blumen and Wu 1995](#)), or time dependency is retained but nonlinearity is not ([Tandon and Garrett 1994](#)). A principal aspect of the solution obtained is the requirement that a , defined below [\(40\)](#), exceed a critical value, unity in the present case, for a frontal discontinuity to form. This formation of a discontinuity in a finite time is a result of a self-advection process contained in [\(50\)](#), or its surrogate [\(41\)](#). Since $f\tau = 1 - \cos ft$ is only a monotonically increasing function of time during the first half of the inertial oscillation, $ft \leq \pi$, a discontinuity will not have sufficient time to form unless the initial relative vorticity exceeds a critical value. Smaller than critical initial relative vorticities lead to undamped inertial oscillations about the evolving geostrophic flow.

Mixed layer restratification following a storm has been examined in some detail by [Tandon and Garrett \(1994, 1995\)](#). Application of the present analysis to this problem is beyond the scope intended, but some comments about their restratification parameter N^2 can be made. This parameter can be interpreted as the buoyancy restoring force in the direction normal to θ surfaces. In momentum coordinates, N^2 may be defined as

where ${}_n g = g \cos \Phi = f^{-1} g \partial \mathbf{v} / \partial z$ using (27). Then introduction of (29a) into (54) yields

$$N^2 = \frac{g}{f} \frac{\partial \mathbf{v}}{\partial Z} \frac{\partial}{\partial X} \frac{\theta}{\theta(0)} \bigg/ \left(1 - \frac{1}{f} \frac{\partial \mathbf{v}}{\partial X} \right). \quad (55)$$

Evaluation of (55) by (33) provides

$$N^2 = M^4 (1 - \cos ft) / f^2 \left(1 - \frac{1}{f} \frac{\partial \mathbf{v}}{\partial X} \right), \quad (56)$$

where $M^4 = (g \partial[\theta/\theta(0)]/\partial X)^2$. At midlevel, where \mathbf{v} vanishes, (56) reduces to the result presented by Tandon and Garrett (1994). The comparison may be extended to the Richardson number defined, for present purposes, as

$$\text{Ri} = N^2 \bigg/ \left[\left(\frac{\partial u^*}{\partial Z} \right)^2 + \left(\frac{\partial \mathbf{v}}{\partial Z} \right)^2 \right]. \quad (57)$$

Evaluation of (57) by (56), (33), and (34) gives

$$\text{Ri} = \frac{1}{2} \left(1 - \frac{1}{f} \frac{\partial \mathbf{v}}{\partial X} \right)^{-1}. \quad (58)$$

Again the Tandon and Garrett result, $\text{Ri} = 1/2$, is recovered at midlevel. The quasi-two-dimensional character of the solutions expressed in momentum coordinates is responsible for the close correspondence between the two results. The relative vorticity, $\partial \mathbf{v} / \partial X$, does not appear in Tandon's and Garrett's result because $\partial[\theta/\theta(0)]/\partial X$ is constant. The appropriate specification of Ri in the present case is, however, determined by use of (36), not (34), and representation in (x, z, t) space. This evaluation need not be carried out here, although Tandon and Garrett note that the presence of low values of $\text{Ri} < 1$ raises the possibility of symmetric instability during restratification. This possibility is excluded, however, in the present model because the potential vorticity cannot become negative.

Acknowledgments

Support for this investigation has been provided by the National Foundation under Grant ATM-9627792. My thanks are expressed to Julie Lundquist for the calculations that appear in the figures.

REFERENCES

- Blumen, W., 1972: Geostrophic adjustment. *Rev. Geophys. Space Phys.*, **10**, 485–528..
- , 1997: A model of inertial oscillations with deformation frontogenesis. *J. Atmos. Sci.*, **54**, 2681–2692.. [Find this article online](#)
- , and R. Wu, 1995: Geostrophic adjustment: Frontogenesis and energy conversion. *J. Phys. Oceanogr.*, **25**, 428–438.. [Find this article online](#)
- Dewar, W. K., and P. D. Killworth, 1995: Do fast gravity waves interact with geostrophic motions? *Deep-Sea Res.*, **42**, 1063–1081..
- Eliassen, A., 1959: On the formation of fronts in the atmosphere. *The Atmosphere and the Sea in Motion*, B. Bolin, Ed., Rockefeller Institute Press, 277–287..
- Hoskins, B. J., and F. P. Bretherton, 1972: Atmospheric frontogenesis models: Mathematical formulation and solution. *J. Atmos. Sci.*, **29**, 11–37.. [Find this article online](#)

—, and I. Draghici, 1977: The forcing of ageostrophic motion according to the semi-geostrophic equations and in an isentropic coordinate model. *J. Atmos. Sci.*, **34**, 1859–1867.. [Find this article online](#)

Houghton, D. D., 1969: Effect of rotation on the formation of hydraulic jumps. *J. Geophys. Res.*, **74**, 1351–1361..

Kuo, A. C., and L. M. Polvani, 1997: Time-dependent fully nonlinear geostrophic adjustment. *J. Phys. Oceanogr.*, **27**, 1614–1634.. [Find this article online](#)

Morse, P. M., and K. U. Ingaard, 1968: *Theoretical Acoustics*. McGraw Hill, 927 pp..

Neves, A. P. C., 1996: Unbalanced frontogenesis with constant uniform potential vorticity. M.S. thesis, 76 pp. [Available from the Dept. of Meteorology, Naval Postgraduate School, Monterey, CA 93943.].

Ou, H. W., 1984: Geostrophic adjustment: A mechanism for frontogenesis. *J. Phys. Oceanogr.*, **14**, 994–1000.. [Find this article online](#)

Platzman, G. P., 1964: An exact integral of complete spectral equations for unsteady one-dimensional flow. *Tellus*, **16**, 422–432..

Rossby, C. G., 1937: On the mutual adjustment of pressure and velocity distribution in simple current systems. *J. Mar. Res.*, **1**, 15–28..

Tandon, A., and C. Garrett, 1994: Mixed layer restratification due to a horizontal density gradient. *J. Phys. Oceanogr.*, **24**, 1419–1424.. [Find this article online](#)

—, and —, 1995: Geostrophic adjustment and restratification of a mixed layer with horizontal gradients above a stratified layer. *J. Phys. Oceanogr.*, **25**, 2229–2241..

APPENDIX

6. Momentum Coordinate Transformation of the Equations

Consider (1), and assume that the pressure gradient force is geostrophically balanced. Then (1) reduces to

$$\frac{\partial u_a}{\partial t} + u_a \frac{\partial u_a}{\partial x} + w \frac{\partial u_a}{\partial z} - f v_a = 0, \quad (\text{A1})$$

where the subscript a denotes the ageostrophic component of the flow. In this model, $u_g = 0$ and $\mathbf{v} = \mathbf{v}_g + \mathbf{v}_a$. Transformation of (A1) into momentum coordinates (6) yields

$$\begin{aligned} \frac{\partial u_a}{\partial T} + u_a \frac{\partial u_a}{\partial X} + w \frac{\partial u_a}{\partial Z} - f v_a + f^{-1} \frac{\partial u_a}{\partial X} \left(\frac{\partial v}{\partial t} + u_a \frac{\partial v}{\partial x} + w \frac{\partial v}{\partial z} \right) \\ = 0. \end{aligned} \quad (\text{A2})$$

Introduction of (2) into (A2) provides (9). A similar procedure provides (10).

The continuity equation (4) is transformed to

$$\frac{\partial u_a}{\partial X} \left(1 + f^{-1} \frac{\partial v}{\partial x} \right) + \frac{\partial w}{\partial Z} + \frac{\partial w}{\partial X} f^{-1} \frac{\partial v}{\partial z} = 0. \quad (\text{A3})$$

The use of (6) also provides

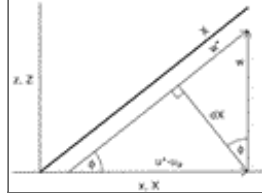
Introduction of (A4) and (A5) into (A3) produces the momentum coordinate representation of the continuity equation, expressed by (11).

Finally, the approach used to derive (9) and (10) transforms (5) into

$$\frac{\partial}{\partial T} \frac{\theta}{\theta(0)} + w \frac{\partial}{\partial Z} \frac{\theta}{\theta(0)} = 0. \quad (\text{A6})$$

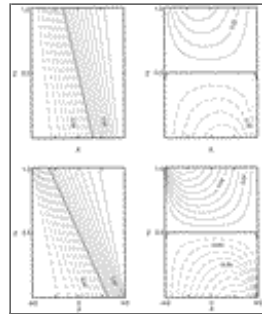
The ZPV condition (7) eliminates the second term, and (A6) reduces to (12).

Figures



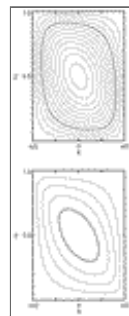
Click on thumbnail for full-sized image.

Fig. 1. Vertical cross sections in the (x, X) – (z, Z) plane. The thick solid line represents an X or θ surface, and dX is normal to X . The velocity variables are defined by (16), the angle Φ by (27), and the interpretation of w^* may be obtained by reference to both (28) and the figure.



Click on thumbnail for full-sized image.

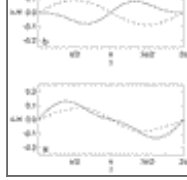
Fig. 2. Left panels: Isotherms in the (x, z) plane for $a = 1$ at times $t = \pi/2$ (top) and $t = \pi$ (bottom). The thick sloping line is $\theta = 0$, and the dashed lines represent $\theta < 0$. Right panels: Contours of alongfront velocity \mathbf{U} (normal to the cross section). The parameter a and times t are as above, and dashed lines represent $\mathbf{U} < 0$.



Click on thumbnail for full-sized image.

Fig. 3. Streamfunctions Ψ in the (x, z) plane corresponding to $a = 1$ and times $t = \pi/2$ and $t = 7\pi/8$. The ageostrophic circulation is counterclockwise. $\Psi = 0$ on the boundaries; the thick solid lines delineate $\Psi = -0.08$, and $\Delta\Psi = 0.02$.





[Click on thumbnail for full-sized image.](#)

Fig. 4. Ageostrophic velocities u (solid) and w (dashed) corresponding to $a = 1$. One inertial oscillation cycle is displayed in (a) $z = 0.25$, (b) $z = 0.50$, and (c) $z = 0.75$.

Corresponding author address: Dr. William Blumen, Program in Atmospheric and Oceanic Sciences, University of Colorado, Campus Box 311, Boulder, CO 80309-0391.

E-mail: blumen@paradox.colorado.edu

[top ▲](#)



© 2008 American Meteorological Society [Privacy Policy and Disclaimer](#)
Headquarters: 45 Beacon Street Boston, MA 02108-3693
DC Office: 1120 G Street, NW, Suite 800 Washington DC, 20005-3826
amsinfo@ametsoc.org Phone: 617-227-2425 Fax: 617-742-8718
[Allen Press, Inc.](#) assists in the online publication of *AMS* journals.